Stochastic Lagrangian Trajectory Model for Drifting Objects in the Ocean

R. Mínguez *, A. J. Abascal *, S. Castanedo *, and R. Medina *

Abstract

The prediction of drifting object trajectories in coastal areas is a complex problem plague of uncertainties. This problem is usually solved simulating the possible trajectories based on wind and currents numerical and/or instrumental data in real time, which are incorporated into Lagrangian trajectory models. However, both data and Lagrangian models are approximations of reality and when comparing trajectory data collected from drifter exercises with respect to Lagrangian models results, they differ considerably. This paper introduces a stochastic Lagrangian trajectory model that allows quantifying the uncertainties related to: i) the wind and currents numerical and/or instrumental data, and ii) the Lagrangian trajectory model. These uncertainties are accounted for within the model through random model parameters. The quantification of these uncertainties consists in an estimation problem, where the parameters of the probability distribution functions of the random variables are estimated based on drifter exercise data. Particularly, it is assumed that estimated parameters maximize the likelihood of our model to reproduce the trajectories from the exercise. Once the probability distribution parameters are estimated, they can be used to simulate different trajectories, obtaining location probability density functions at different times. The advantage of this method is that it allows: i) site specific calibration, and ii) comparing uncertainties related to different wind and currents predictive tools. The proposed method is applied to data collected during the DRIFTER Project (eranet AMPERA, VI Programa Marco), showing very good predictive skills.

Key words: Drifter exercise, Drifting objects, Lagrangian trajectory model, Stochastic trajectory model

* Environmental Hydraulics Institute "IH Cantabria", Universidad de Cantabria, Cantabria, Spain

Email address: Roberto.Minguez@unican.es (R. Mínguez).

1 Introduction

The transport of objects and substances by surface currents, wind, wave fields and turbulence, commonly referred to as drift, is very important from the human perspective for solving problems such as, forecasting the evolution of oil spills, tracking of elements which may be a threat to maritime safety, search-and-rescue of humans and/or ships, backtracking looking for ships responsible of illicit flushing of ballast tanks, etc.

Models for drifting objects are quite complex (Spaulding et al., 1992; Beegle-Krause, 1999; Daniel et al., 2003; Castanedo et al., 2006). There are two main reasons: i) they involve different interacting processes which are difficult to reproduce, and ii) the difficulties of determining the current status of the object itself and the ocean. Note that the movement of the drifting object is induced by variables such as, winds, currents, and waves acting on the object, and thus the importante on the knowledge of these parameters.

An additional challenge when predicting the drift of objects on the sea surface is how to account for the uncertainties inherent in almost all aspects of the problem (Hackett et al., 2005):

(1) Most formulations are based on empirical parameterizations, and approximations of the hydrodynamical laws.
(2) Wind, wave and current data used to drive the model are subject to a great amount of uncertainty. Note that weather forecasts have good predictive skill for periods up to 3-4 days, which degrades gradually as time goes by.
(3) The orientation of the object with regard to the local wind direction. Whether the object drifts to the left or to the right of the wind cannot be known in advance and unless more is known about the object we must assign equal probability to the two outcomes.

The best way of accounting for uncertainty is using an stochastic framework. The relevant parameters are considered random variables and their uncertainty is quantified in terms of a probability distribution function. Thus, using Monte Carlo method (Rubinstein, 1981) it is possible to simulate multiple trajectories, getting a cloud of candidate locations for the drifting object. These locations allow identifying the evolution of the most likely positions of the drifting object in time. A discussion of more advanced stochastic methods can be found in Griffa (1996) and Berloff and McWilliams (2002). Obviously, i) the choice of the initial random model parameters, ii) their distribution, and iii) their parameter estimation is of paramount importance, affecting the future search area seriously.

The advantage of dealing with uncertainty when predicting the drift of objects

is that simple models, representing the most important physical processes, may be used instead of complex and sophisticated models. In these cases, the appropriate definition of the uncertainty is more important than the complexity of the model itself, and they may provide equally or better results.

Several studies have been carried out in the literature to take into account the different sources of uncertainty in the trajectory simulations. An attempt to quantify and calculate the uncertainties of a predictive model for oil spill trajectories is given in Sebastião and Guedes Soares (2006), for coastal zones, and Sebastião and Guedes Soares (2007), for open sea. Note that in both articles the same stochastic model is proposed, predicting the uncertainty of the oil spill trajectory from the uncertainties of the input parameters. The model considers the output as a function of the random variables, i.e. input parameters, and calculates the standard deviation of the output results as a function of the standard deviation of the input parameters.

Rixen and Ferreira-Coelho (2007) developed a methodology to forecast at short time scale Lagrangian drifts from combined atmospheric and ocean operational models and local observations using linear and nonlinear statistics. In that work, the authors propose a method to solve the surface drift problem using linear and non-linear regression techniques, namely neural networks and genetic algorithms. Rixen et al. (2008) apply the methodology in the Adriatic Sea and discuss the performance of the hyper-ensembles and the individual models by analyzing associated uncertainties and probability distribution maps for drifter positions.

Abascal et al. (2009b) introduce a methodology to calibrate a Lagragian trajectory model by means of an automatic method. The aim of their work is to find the optimal values of the model coefficients that minimize the differences between numerical and actual trajectories provided by drifter observations. In that work, the authors show the importance of obtaining the best agreement model coefficients for the study area in order to provide the most accurate trajectory simulations. In a later study, Abascal et al. (2009a) propose a methodology to optimize the transport model performance and to calculate the search area of the predicted positions. In their methodology, the transport model is calibrated by means of a global optimization algorithm, which allows obtaining the optimal model parameters and their corresponding 95% confidence intervals. Subsequently, the calibration results are used to compute the buoy trajectory using Monte Carlo simulation. Finally, the 95% confidence areas are determined by means of a bivariate kernel estimator. The methodology is applied and validated using data from drifting buoys.

Previous models present several deficiencies. In the model proposed by Sebastião and Guedes Soares (2006, 2007):

- The random model parameters are assumed to be normally distributed, i.e. mean and standard deviation parameters are enough to define the probability distribution. And it is difficult to relax that assumption.
- It uses a first-order Taylor series expansion around the expected trajectory, which is a non-linear function of the input parameters. Note that the method proposed by Sebastião and Guedes Soares (2006, 2007) is a particular instance, i.e. the simplest, of point-estimate methods. These methods approximate the description of the statistical properties of the output random variables of a problem using commonly available information on the random behavior of input variables, such as their first statistical moments (e.g., mean, variance and skewness) (Rosenblueth, 1975; Harr, 1989; Hong, 1998; Morales and Pérez-Ruiz, 2007).
- The standard deviations used are not based on data for the particular location. They are selected by introducing different perturbations on the mean values, which are based on estimates from other stochastic approaches.

The model by Rixen and Ferreira-Coelho (2007); Rixen et al. (2008) quantifies the uncertainty related to different ensembles using complex nonlinear regression models which must be solved through neuronal networks and genetic algorithms. These makes the model fuzzy and difficult to implement.

Regarding the models proposed by Abascal et al. (2009b,a):

- The parameters are assumed to follow different probability distribution functions and there are several model parameters, which are calibrated by minimizing the differences between numerical and actual trajectories provided by drifter observations. Note that the parameter calibration problem and the estimation of the probability distribution parameters, which are usually taken from other studies, are decoupled.
- The calibration consist of a least squares estimation problem, that corresponds to the maximum likelihood estimates only if the parameters are normally distributed, which is not the case.
- The 95% confidence intervals from Monte Carlo simulations still do not contain the actual trajectories, showing that the uncertainty is not properly modeled.

This paper tries to solve all these shortcomings for those situations where there exist available historical information about drifting object trajectories. Thus, the aim of the paper is threefold: i) to present a simple but realistic stochastic Lagrangian model for trajectory evolution, ii) to estimate the random model parameters based on data from drifter exercises, so that estimated parameters maximize the likelihood of our model to reproduce the trajectories from the exercise, and iii) to obtain, based on Monte Carlo simulations, the location probability density functions of the drifter object at different times.

The rest of the paper is organized as follows. Section 2 i) presents the stochastic Lagrangian model for trajectory evolution, ii) provides the description of the estimation method based on the maximum likelihood principle, and iii) analyses the study of temporal correlation between random model parameters. In Section 3, the Monte Carlo simulation method including temporal autocorrelation is explained. In section 4, the model, estimation and simulations are applied using data from the "DRIFTER Project" (eranet AMPERA, VI Programa Marco). Finally, Section 5 provides some relevant conclusions.

2 Stochastic Lagrangian model

A drifting object on the sea surface moves due to the net result of several forces (water currents, atmospheric wind, wave motion, and turbulence dispersion). This movement is governed by the diffusion and advection transport equation in Lagrangian form, i.e.:

$$\frac{d\boldsymbol{x}}{dt} = \boldsymbol{U}_a(\boldsymbol{x}, t) + \boldsymbol{U}_s(\boldsymbol{x}, t), \tag{1}$$

where $\boldsymbol{x} = (x, y)$ is the positioning vector, and $\boldsymbol{U}_a$ and $\boldsymbol{U}_s$ are advection and diffusion velocity vectors, respectively. Note that both positioning and velocities are time t dependent processes.

The advection velocity $\boldsymbol{U}_a$ can be expressed as a linear combination of surface currents (Ekman drift, baroclinic motion, tidal and inertial currents), leeway velocity due to wind, and Stokes drift induced by waves:

$$\boldsymbol{U}_a(\boldsymbol{x}, t) = \boldsymbol{U}_C(\boldsymbol{x}, t) + C_D\boldsymbol{U}_W(\boldsymbol{x}, t) + C_H\boldsymbol{U}_H(\boldsymbol{x}, t), \tag{2}$$

where $\boldsymbol{U}_C$ is the surface current velocity vector, $\boldsymbol{U}_W$ is the wind velocity at 10 meters height, and $\boldsymbol{U}_H$ is wave-induced Stokes drift velocity. C_D and C_H correspond to the leeway and Stokes coefficients, respectively. Note that traditionally, the advection term is assumed to be deterministic, where the optimal parameters C_D and C_H are between 3-3.5% (ASCE, 1996) and 0.05-1.5% (Castanedo et al., 2006). However, in this paper, coefficients C_D and C_H are assumed to be normally distributed random variables with parameters $(\mu_{C_D}, \sigma^2_{C_D})$ and $(\mu_{C_H}, \sigma^2_{C_H})$, respectively.

In addition, the diffusive velocity $\boldsymbol{U}_s$ is also assumed to be stochastic. There are two random spreading components: longitudinal D_L and transversal D_T. These components are related to the direction of the advection velocity $\boldsymbol{U}_a$. Assuming that the angle between the advection velocity and the abscissas axis

is γ, the velocity $\boldsymbol{U}_s$ in the reference coordinate system is given by:

$$\boldsymbol{U}_s = \begin{pmatrix} \cos\gamma & -\sin\gamma \\ \sin\gamma & \cos\gamma \end{pmatrix} \begin{pmatrix} D_L \\ D_T \end{pmatrix}, \tag{3}$$

where both D_L and D_T are normally distributed random variables with parameters $(\mu_{D_L}, \sigma^2_{D_L})$ and $(\mu_{D_T}, \sigma^2_{D_T})$, respectively.

2.1 Numerical scheme

Note that the equation (1) governs the response and movement of the drifting object. The evolution of the location is obtained solving this ordinary differential equation (ODE) under the following assumptions:

(1) The initial location of the drifting object is known (initial condition).
(2) Currents, wind speeds and waves information is given at regular time intervals Δt.

The selected numerical method to solve (1) is the first-order Euler method, where the location of the drifting object is defined as:

$$\begin{aligned} \boldsymbol{x}_t &= \boldsymbol{x}_{t-1} + \Delta t \left[\boldsymbol{U}_a(\boldsymbol{x}_{t-1}) + \boldsymbol{U}_s(\boldsymbol{x}_{t-1})\right] \\ &= \boldsymbol{x}_{t-1} + \Delta t \Big[\boldsymbol{U}_C(\boldsymbol{x}_{t-1}) + C_D^{t-1}\boldsymbol{U}_W(\boldsymbol{x}_{t-1}) + \dots \\ &\quad C_H^{t-1}\boldsymbol{U}_H(\boldsymbol{x}_{t-1}) + \boldsymbol{U}_s(\boldsymbol{x}_{t-1})\Big]\ ;\ t = 1, \dots, n_t, \end{aligned} \tag{4}$$

where $\boldsymbol{x}_t$ is the location of the drifting object at time t, $\boldsymbol{U}_a(\boldsymbol{x}_t)$, $\boldsymbol{U}_s(\boldsymbol{x}_t)$, $\boldsymbol{U}_C(\boldsymbol{x}_t)$, $\boldsymbol{U}_W(\boldsymbol{x}_t)$, and $\boldsymbol{U}_H(\boldsymbol{x}_t)$ are, respectively, the advection, the diffusion, the surface current, the wind at 10 meters height, and the Stokes drift velocities at the location of the object at time t, i.e. $\boldsymbol{x}_t$. Parameters C_D^t and C_H^t are the leeway and Stokes coefficients at the location of the object at time t, respectively, and n_t is the number of time intervals considered. Using (3), the diffusion velocity can be expressed as:

$$\boldsymbol{U}_s(\boldsymbol{x}_{t-1}) = \begin{pmatrix} \cos(\gamma_{t-1}) & -\sin(\gamma_{t-1}) \\ \sin(\gamma_{t-1}) & \cos(\gamma_{t-1}) \end{pmatrix} \begin{pmatrix} D_L^{t-1} \\ D_T^{t-1} \end{pmatrix}, \tag{5}$$

where γ_{t-1} is the direction angle of the advection velocity $\boldsymbol{U}_a(\boldsymbol{x}_{t-1})$, and D_L^t and D_T^t are the longitudinal and transversal diffusion velocities at the location of the object at time t.

Note that C_D^t, C_H^t, D_L^t, and D_T^t are random model variables, which we assume that follow a normal distribution with parameters $(\mu_{C_D}, \sigma^2_{C_D})$, $(\mu_{C_H}, \sigma^2_{C_H})$, $(\mu_{D_L}, \sigma^2_{D_L})$ and $(\mu_{D_T}, \sigma^2_{D_T})$, respectively. An advantage of the proposed procedure is that alternative distributions, such as log-normal, uniform, etc. could be used instead. Note also that these random model parameters also account, implicitly, for the uncertainties of the numerical scheme. However, alternative formulations including more complex parameterizations or numerical schemes are possible. The adequacy of the model must be established based on the estimation results, which should follow the selected probability distribution hypothesis.

2.2 The Maximum Likelihood Method

The maximum likelihood method is based on maximizing the likelihood of an observed sample, and it can be used to derive point and interval parameter estimates.

In this particular case, the observed sample corresponds to the trajectories obtained from a drifter exercise, or from the evolution of an oil spill using satellite images, etc. We assume that the random probability distribution parameters $(\mu_{C_D}, \sigma^2_{C_D})$, $(\mu_{C_H}, \sigma^2_{C_H})$, $(\mu_{D_L}, \sigma^2_{D_L})$ and $(\mu_{D_T}, \sigma^2_{D_T})$ are estimated so that, using Euler approach (4), the likelihood of the model to reproduce the given trajectories is maximized.

Being n_d the number of drifting objects, and assuming that: i) the random model variables are independent, and ii) the locations of the i-th object $\boldsymbol{x}_t^i;\ t = 0, \ldots, n_t,\ i = 0, \ldots, n_d$ at different times are given, the mean and standard deviation parameters $\boldsymbol{\theta} = (\mu_{C_D}, \sigma_{C_D},\ \mu_{C_H}, \sigma_{C_H},\ \mu_{D_L}, \sigma_{D_L},\ \mu_{D_T}, \sigma_{D_T})^T$ can be estimated using the loglikelihood function by solving the following optimization problem:

$$\underset{\boldsymbol{\theta}, C_D^{i,t}, C_H^{i,t}, D_L^{i,t}, D_T^{i,t}}{\text{Maximize}} \left\{ \begin{array}{l} \displaystyle\sum_{t=1}^{n_t}\sum_{i=1}^{n_d} \log\left[f_{C_D}(C_D^{i,t};\boldsymbol{\theta})\right] + \sum_{t=1}^{n_t}\sum_{i=1}^{n_d} \log\left[f_{C_H}(C_H^{i,t};\boldsymbol{\theta})\right] + \\ \displaystyle\sum_{t=1}^{n_t}\sum_{i=1}^{n_d} \log\left[f_{D_L}(D_L^{i,t};\boldsymbol{\theta})\right] + \sum_{t=1}^{n_t}\sum_{i=1}^{n_d} \log\left[f_{D_T}(D_T^{i,t};\boldsymbol{\theta})\right] \end{array} \right\} \quad (6)$$

subject to

$$\boldsymbol{x}_t^i - \boldsymbol{x}_{t-1}^i = \Delta t \left[\boldsymbol{U}_a(\boldsymbol{x}_{t-1}^i) + \boldsymbol{U}_s(\boldsymbol{x}_{t-1}^i)\right];\ t = 1, \ldots, n_t;\ i = 1, \ldots, n_d \quad (7)$$

$$\boldsymbol{U}_a(\boldsymbol{x}_{t-1}^i) = \boldsymbol{U}_C(\boldsymbol{x}_{t-1}^i) + C_D^{i,t-1}\boldsymbol{U}_W(\boldsymbol{x}_{t-1}^i) + C_H^{i,t-1}\boldsymbol{U}_H(\boldsymbol{x}_{t-1}^i);\ \forall t;\ \forall i \quad (8)$$

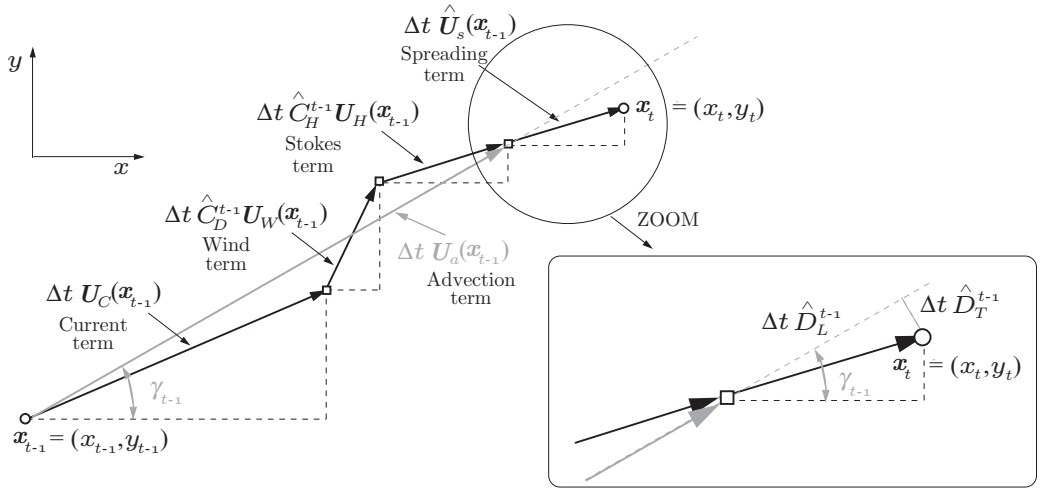

Fig. 1. Graphical interpretation of the estimated values of the random variables and constraints (7)-(10), which allow reproducing the given trajectory.

$$\gamma_{t-1}^i = \arctan\left(\frac{U_{a_y}^i}{U_{a_x}^i}\right);\ t = 1, \ldots, n_t;\ i = 1, \ldots, n_d \tag{9}$$

$$\boldsymbol{U}_s(\boldsymbol{x}_{t-1}^i) = \begin{pmatrix} \cos\left(\gamma_{t-1}^i\right) & -\sin\left(\gamma_{t-1}^i\right) \\ \sin\left(\gamma_{t-1}^i\right) & \cos\left(\gamma_{t-1}^i\right) \end{pmatrix} \begin{pmatrix} D_L^{i,t-1} \\ D_T^{i,t-1} \end{pmatrix};\ \forall t;\ \forall i \tag{10}$$

$$\sigma_{C_D} > 0 \tag{11}$$

$$\sigma_{C_H} > 0 \tag{12}$$

$$\sigma_{D_L} > 0 \tag{13}$$

$$\sigma_{D_T} > 0, \tag{14}$$

where f_{C_D}, f_{C_H}, f_{D_L} and f_{D_T} are the probability density functions of the corresponding random variables, and $\boldsymbol{x}_t^i$ are the data locations related to the ith trajectory (drifting object). Note that problem (6)-(14) differs from the traditional maximum likelihood formulation because the actual values of the random variables are unknown and must be obtained from the trajectory equations (7)-(10). The optimal value obtained from solving problem (6)-(14), i.e. $\hat{\boldsymbol{\theta}}$, is the *maximum likelihood estimate* (MLE) of $\boldsymbol{\theta}$. In addition, the most likely values of the random variables $(\hat{C}_D^{i,t}, \hat{C}_H^{i,t}, \hat{D}_L^{i,t}, \hat{D}_T^{i,t};\ t = 0, \ldots, n_t - 1;\ i = 0, \ldots, n_d)$ are also obtained. These values represent the values of the random variables which allows reproducing the given trajectory with maximum probability. In Figure 1, the graphical interpretation of the variables and constraints (7)-(10), related to the Euler method, is illustrated.

Observe that the maximization of the log-likelihood function can be done using any of the available solvers for nonlinear programming subject to constraints and bounds on variables, for instance, solver MINOS (Murtagh and Saunders, 1998) under GAMS (Brooke et al., 1998) which allows for upper and lower bounds on parameters to be estimated and dealing with nonlinear equality

constraints, and uses a reduced-gradient algorithm (Wolfe, 1963) combined with the quasi-Newton algorithm given in Murtagh and Saunders (1978), or the Trust Region Reflective Algorithm under Matlab (Coleman and Li, 1994, 1996), also capable of dealing with nonlinear equality constraints and upper and lower bounds through the function `fmincon`.

The advantage of using the maximum likelihood method is that all consistent solutions are asymptotically normally distributed, that is,

$$\hat{\boldsymbol{\theta}} \rightarrow N_k\left(\hat{\boldsymbol{\theta}}, \Sigma_{\hat{\boldsymbol{\theta}}}\right), \tag{15}$$

where $N_k\left(\hat{\boldsymbol{\theta}}, \Sigma_{\hat{\boldsymbol{\theta}}}\right)$ denotes the k-dimensional normal distribution with mean vector $\hat{\boldsymbol{\theta}}$ and covariance matrix $\Sigma_{\hat{\boldsymbol{\theta}}}$. The covariance matrix $\Sigma_{\hat{\theta}}$ is the inverse of the Fisher *information matrix*, $\mathbf{I}_\theta$, whose (r, j)th element is given by

$$i_{rj} = -\left.\frac{\partial^2 \ell(\theta|x)}{\partial\theta_r \partial\theta_j}\right|_{\theta=\hat{\theta}}. \tag{16}$$

In addition, the probability density functions may correspond to any kind of random variable distribution, such as normal, lognormal, uniform, exponential, etc. For this particular case, we assume normal random variables:

$$f_X(x) = \frac{1}{\sqrt{2\pi\sigma^2}} e^{-\frac{(x-\mu)^2}{2\sigma^2}}. \tag{17}$$

The main advantage of this method is that it allows the calculation of the probability distribution parameters based on observed data. This feature makes it appropriate for comparing different wind, wave and current prediction technologies. Note, for instance, that we could solve (6)-(14) using different current information $\boldsymbol{U}_C(\boldsymbol{x}_t)$ sources, such as numerical forecasting modelling or HF radar measurements. The method provides a rationale criterion for comparing their performance.

2.3 Temporal dependence

The parameter estimation method presented in the previous section assumes temporal independence related to the random variables $C_D^{i,t}$, $C_H^{i,t}$, $D_L^{i,t}$, and $D_T^{i,t}$. We advocate this approach due to its simplicity and practical performance. However, the most likely values of the random variables, i.e. $\hat{C}_D^{i,t}$, $\hat{C}_H^{i,t}$, $\hat{D}_L^{i,t}$, $\hat{D}_T^{i,t}$ may hide a temporal dependency structure which could be further explored after the parameter estimation.

Autoregressive moving average ARMA(p, q) processes are time dependent models specially suitable to explore temporal dependencies. These models can be mathematically expressed as

$$y_t = \sum_{j=1}^{p} \phi_j y_{t-j} + \varepsilon_t - \sum_{j=1}^{q} \theta_j \varepsilon_{t-j} \tag{18}$$

with p autoregressive parameters ϕ_1, ϕ_2, ..., ϕ_p, and q moving average parameters θ_1, θ_2, ..., θ_q. The term ε_t in equation (18) stands for an uncorrelated normal stochastic process with mean zero and variance σ_ε^2, and is also uncorrelated with $y_{t-1}, y_{t-2}, \ldots, y_{t-p}$. Stochastic process ε_t is also referred to as *white noise*, *innovation term*, or *error term*.

Observe in (18) that y_t boils down to a linear combination of white noises, and as such, the marginal distribution associated with the stochastic process $\boldsymbol{Y}$ is necessarily normal. In order to preserve the original marginal distribution associated with the random model variables while making use of the modeling capability of the ARMA models, new stochastic process, $\boldsymbol{Z}$, with a standard normal marginal distribution is defined through the following transformation (Liu and Der Kiureghian, 1986):

$$\boldsymbol{Z} = \Phi^{-1}\left[F_Y(\boldsymbol{Y})\right], \tag{19}$$

where F_Y is the cumulative distribution function (CDF) of the marginal distribution associated with the original stochastic process $\boldsymbol{Y}$ and $\Phi(\cdot)$ is the cumulative distribution function of the standard normal random variable.

Thus, the stochastic temporal dependence of the random variables C_D^t, C_H^t, D_L^t, D_T^t is reproduced using transformation (19) and the following univariate ARMA models:

$$z_t^{C_D} = \sum_{j=1}^{p^{C_D}} \phi_j^{C_D} z_{t-j}^{C_D} + \varepsilon_t^{C_D} - \sum_{j=1}^{q^{C_D}} \theta_j^{C_D} \varepsilon_{t-j}^{C_D} \tag{20}$$

$$z_t^{C_H} = \sum_{j=1}^{p^{C_H}} \phi_j^{C_H} z_{t-j}^{C_H} + \varepsilon_t^{C_H} - \sum_{j=1}^{q^{C_H}} \theta_j^{C_H} \varepsilon_{t-j}^{C_H} \tag{21}$$

$$z_t^{D_L} = \sum_{j=1}^{p^{D_L}} \phi_j^{D_L} z_{t-j}^{D_L} + \varepsilon_t^{D_L} - \sum_{j=1}^{q^{D_L}} \theta_j^{D_L} \varepsilon_{t-j}^{D_L} \tag{22}$$

$$z_t^{D_T} = \sum_{j=1}^{p^{D_T}} \phi_j^{D_T} z_{t-j}^{D_T} + \varepsilon_t^{D_T} - \sum_{j=1}^{q^{D_T}} \theta_j^{D_T} \varepsilon_{t-j}^{D_T}. \tag{23}$$

One advantage of this kind of models is that well-known and computationally

efficient univariate modeling procedures can be employed to estimate model parameters in (20)-(23). Note also that residuals are uncorrelated $E[\varepsilon_t^{C_D}\varepsilon_{t-j}^{C_D}] = 0$, $E[\varepsilon_t^{C_H}\varepsilon_{t-j}^{C_H}] = 0$, $E[\varepsilon_t^{D_L}\varepsilon_{t-j}^{D_L}] = 0$ and $E[\varepsilon_t^{D_T}\varepsilon_{t-j}^{D_T}] = 0$.

The standard protocol for model selection and parameter estimation can be found in Box et al. (1994).

Once the model parameters in (20)-(23) are estimated, it is possible to reproduce not only the marginal distribution related to the random model variables, but also its temporal dependency. This characteristic is used afterwards for the simulation of new trajectories.

2.4 Hypothesis testing

The model proposed in this paper has the advantage that it can be combined with any kind of probability density function. For this reason, once the parameter estimation processes given in subsections 2.2 and 2.3 are accomplished, it is very important to run different statistical hypothesis tests to check whether the selected distributions were appropriate or not. In this particular case we use the following tests:

- Related to the marginal probability distribution function selected for the random model variables, a one-sample Kolmogorov-Smirnov test (Massey (1951)) is performed. This test compares for a given significance level α the transformed values $z_t^{C_D}$, $z_t^{C_H}$, $z_t^{D_L}$, $z_t^{D_T}$ using (19) with respect to a standard normal distribution. The null hypothesis is that the samples follow a standard normal distribution.
- Analogously to the previous case, we perform a one-sample Kolmogorov-Smirnov test for residuals divided by their standard deviation estimates. The null hypothesis is that they follow a standard normal distribution.
- Related to the temporal dependence of the stochastic variables, the following tests and diagnostic plots are selected:

(1) Sample autocorrelation and partial autocorrelation functions related to the transformed values $z_t^{C_D}$, $z_t^{C_H}$, $z_t^{D_L}$, $z_t^{D_T}$. These plots help deciding the orders p and q of the ARMA processes.
(2) Sample autocorrelation and partial autocorrelation functions related to the estimated residuals $\varepsilon_t^{C_D}$, $\varepsilon_t^{C_H}$, $\varepsilon_t^{D_L}$, $\varepsilon_t^{D_T}$. Since the residuals are supposed to be uncorrelated, these values should be within the confidence bounds.
(3) To further explore the residuals independence hypothesis, the Ljung-Box lack-of-fit hypothesis test (Brockwell and Davis, 1991) for model misidentification is applied. This test indicates the acceptance or not of the null hypothesis that the model fit is adequate (no serial correlation at the

corresponding element of Lags).

Additional or alternative tests for those selected above could be applied. Note that in case any of those tests allow rejecting the null hypothesis with a given significance level, the probability distribution assumptions must be revisited before being acceptable for simulation purposes.

3 Monte Carlo trajectory simulation

Once the relevant parameters of the model are estimated, it is possible to use the Monte Carlo method (Rubinstein, 1981) in conjunction with the joint probability distribution function and the temporal dependency model presented in the previous section, to simulate multiple trajectories, getting a cloud of candidate locations for the drifting object.

In this section, the procedure to generate those trajectories is described step by step.

Algorithm 3.1 (Trajectory simulation).

Input: Maximum likelihood estimated parameters $\hat{\boldsymbol{\theta}}$, the estimates of the ARMA models defined in (20)-(23) and the standard deviation of the corresponding residuals, i.e. $\sigma_{\varepsilon}^{C_D}$, $\sigma_{\varepsilon}^{C_H}$, $\sigma_{\varepsilon}^{D_L}$, $\sigma_{\varepsilon}^{D_T}$, the initial location of the drifting object $\boldsymbol{x}_0$, the Euler time step Δt, the predicted velocity currents and finally, the number of trajectories n_s and time steps t_s to be simulated.

Step 1: Initialization. Set the iteration counter to $\nu = 1$ and go to Step 2.

Step 2: Error simulation. Simulate the vectors $\tilde{\boldsymbol{\varepsilon}}^{C_D}$, $\tilde{\boldsymbol{\varepsilon}}^{C_H}$, $\tilde{\boldsymbol{\varepsilon}}^{D_L}$, $\tilde{\boldsymbol{\varepsilon}}^{D_T}$ of dimensions $t_s \times 1$ composed by independent normal random errors with standard deviations $\sigma_{\varepsilon}^{C_D}$, $\sigma_{\varepsilon}^{C_H}$, $\sigma_{\varepsilon}^{D_L}$, $\sigma_{\varepsilon}^{D_T}$, respectively. Note that the tilde refers to simulated values.

Step 3: ARMA. Use those simulated errors in the ARMA models given in (20)-(23) obtaining the vectors $\tilde{\boldsymbol{z}}^{C_D}$, $\tilde{\boldsymbol{z}}^{C_H}$, $\tilde{\boldsymbol{z}}^{D_L}$, and $\tilde{\boldsymbol{z}}^{D_T}$.

Step 4: Inverse transformation. Get the simulated values of the random model variables, i.e. $\tilde{\boldsymbol{C}}_D$, $\tilde{\boldsymbol{C}}_H$, $\tilde{\boldsymbol{D}}_L$, and $\tilde{\boldsymbol{D}}_T$, using the inverse of transformation (19).

Step 5: Trajectory generation. Reproduce the simulated trajectory through the Euler method given in (4). Update the iteration counter $\nu \rightarrow \nu + 1$, if $\nu \leq n_s$ go to Step 2 otherwise the trajectory simulation process concludes.

■

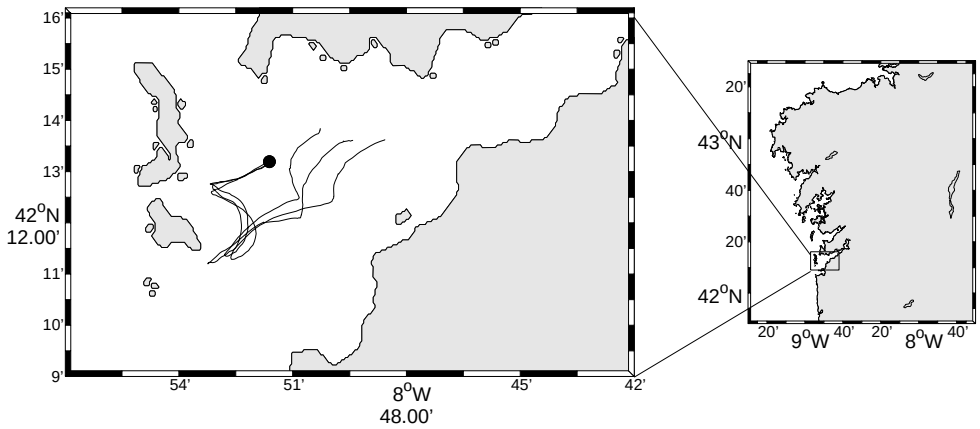

Fig. 2. Study area and buoys trajectories. The black circle represents the buoys deployment. The buoys trajectories span from September 14th 9:30 UTC to September 15th 17:00 UTC approximately.

4 Case study: application to drifting buoys

The methodology has been applied to simulate the trajectory of drifting buoys in the Bay of Vigo (Galicia, Spain) (see Figure 2). Data used were collected during an exercise developed within the framework of the aforementioned DRIFTER project (AMPERA, ERA-net VI European Framework Programme). As part of the project, several sets of experiments were carried out by INTECMAR (Instituto Tecnológico para el Control del Medio Marino de Galicia) in order to study the influence of ocean-meteorological conditions and buoys features on the drifting trajectory (http://www.intecmar.org/drifter/). During one of these exercises a set of 13 buoys were released in the Bay of Vigo (Galicia, Spain) between September 14th 2010 and September 15th 2010 (Allen-Perkins et al., 2010). All the buoys provided a 15 minute sampling rate of their positions.

In this paper we only analyze three of the thirteen trajectories. Figure 2 shows the study area and the path followed by the buoys used for the present study. We consider two different time periods:

(1) From September 14th 2010 at 09:30:00 to September 14th 2010 at 15:45:00 in 15 minute intervals. This period is used for the parameter estimation processes.

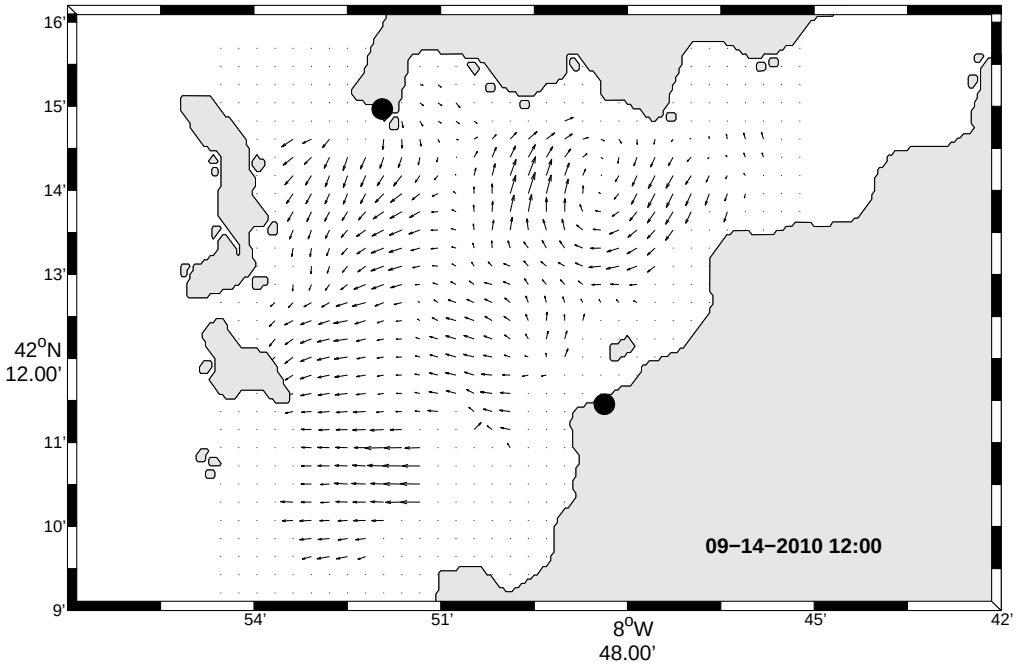

Fig. 3. Typical surface current map provided by the high-resolution Bay of Vigo coastal HF radar system of the University of Vigo. The radar site locations are indicated by solid black circles

(2) From September 14th 2010 at 15:45:00 to September 14th 2010 at 22:00:00. This period is used for validation, checking how the simulated trajectories contain the actual buoy trajectories.

The trajectories were simulated using, as forcing of the stochastic model, surface currents measured by HF radar currents. Previous studies showed that buoy trajectories analyzed in this work could be simulated using only HF radar currents as forcing (Abascal et al., 2011a,b).

HF radar surface currents were provided by the high-resolution HF radar network at the Bay of Vigo owned and operated by University of Vigo (Varela, 2010). The HF radar network consists of two CODAR systems which provided 30 min surface currents at 400 m horizontal resolution in the Bay of Vigo. A typical total vector plot for this system is shown in Figure 3. During the radar exercise, there was a problem with the power supply which led to a gap in the total surface currents for the period between September 14th 2010 22:30 and September 15th 2010 08:00 UTC. This fact prevents us from using all the trajectory information at our disposal.

Table 1
Maximum likelihood estimates and 95% confidence intervals of the D_T and D_L random variable probability distributions.

Parameter	Lower bound	Mean	Upper bound
$\hat{\mu}_{D_T}$(m/s)	0.0092542	0.0182416	0.0272290
$\hat{\sigma}_{D_T}$(m/s)	0.0271324	0.0373128	0.0474932
$\hat{\mu}_{D_L}$(m/s)	0.0044360	0.0107911	0.0171461
$\hat{\sigma}_{D_L}$(m/s)	0.0350671	0.0422657	0.0494643

4.1 Parameter estimation process

The first step consists in estimating the parameters of the longitudinal D_L and transversal D_T random diffusive components. Note that no information about winds and waves was used. This is a subject for further research.

The maximum likelihood estimates using the three trajectory data from September 14th 2010 at 09:30:00 to September 14th 2010 at 15:45:00 are given in Table 1. Note that only the probability distribution parameters related to the variables D_T and D_L, respectively, are provided. The units are in meters per second. An interesting result is the magnitude of the standard deviations related to the transversal and longitudinal diffusion velocities, which are similar (0.037 versus 0.042) and assuming a 15 minute time interval it corresponds to $\approx$ 36 meters of diffusion uncertainties. This result is not consistent with the traditional assumption that the longitudinal diffusion uncertainty is one order of magnitude higher than the transversal diffusion uncertainty.

In Figure 4, the three trajectories used for the MLE parameter estimation process, labeled as Data 1, 2, and 3, respectively, are shown (black and gray scale circle marker specifiers). In addition, the trajectories obtained considering only the current velocity, labeled as deterministic trajectories, are also shown. Note that the MLE estimation process provides the values of the random variables $\hat{\boldsymbol{D}}_T$ and $\hat{\boldsymbol{D}}_L$ which allows reproducing the data trajectories. Note that these trajectories are plotted using red, blue and green circle marker specifiers, respectively, and they coincide with the trajectory data. This is the target of the proposed parameter estimation method.

In order to check the normal random marginal probability distributions assumed for both D_T and D_L random variables, we transform $\hat{\boldsymbol{D}}_T$ and $\hat{\boldsymbol{D}}_L$ using

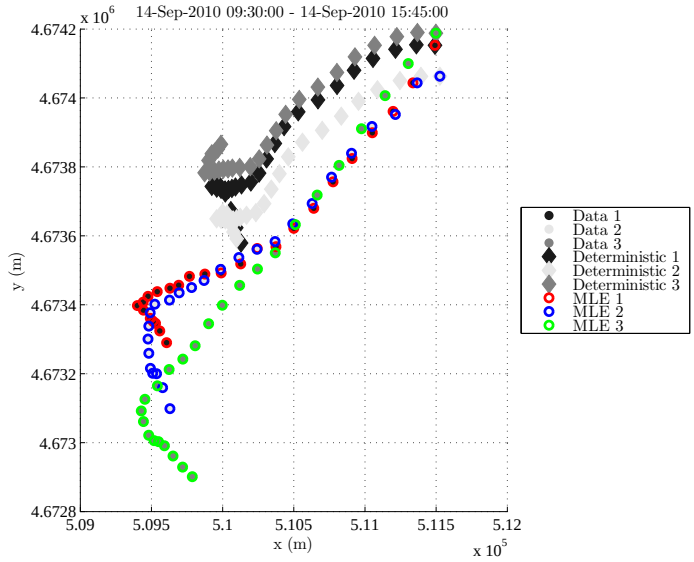

Fig. 4. Selected trajectories for the MLE estimation problem, and deterministic and final MLE trajectories.

(19), which in this case becomes:

$$\begin{aligned} \hat{\boldsymbol{z}}^{D_T} &= \frac{\hat{\boldsymbol{D}}_T - \hat{\mu}_{D_T}}{\hat{\sigma}_{D_T}} \\ \hat{\boldsymbol{z}}^{D_L} &= \frac{\hat{\boldsymbol{D}}_L - \hat{\mu}_{D_L}}{\hat{\sigma}_{D_L}}, \end{aligned} \tag{24}$$

and, afterwards, we apply the one-sample Kolmogorov-Smirnov test with 0.05 significance level for both samples. Note that the p-values obtained are 0.1791 and 0.41992, respectively, so that the null hypothesis that both samples follow a standard normal distribution is accepted. In addition, Figure 5 shows the histograms and normal probability plots of the maximum likelihood estimates $\hat{D}_T^t$ and $\hat{D}_L^t$, which present good agreement with respect to the normal distributions.

4.2 Temporal dependence

To further investigate the possible temporal dependence on the stochastic processes related to the variables D_T^t and D_L^t, the autocorrelation and partial autocorrelation functions related to the maximum likelihood values of the random variables $\hat{z}_t^{D_T}$ (panels above) and $\hat{z}_t^{D_L}$ (panels below) are shown in Figure 6.

Note that in both processes the autocorrelation function decays gradually,

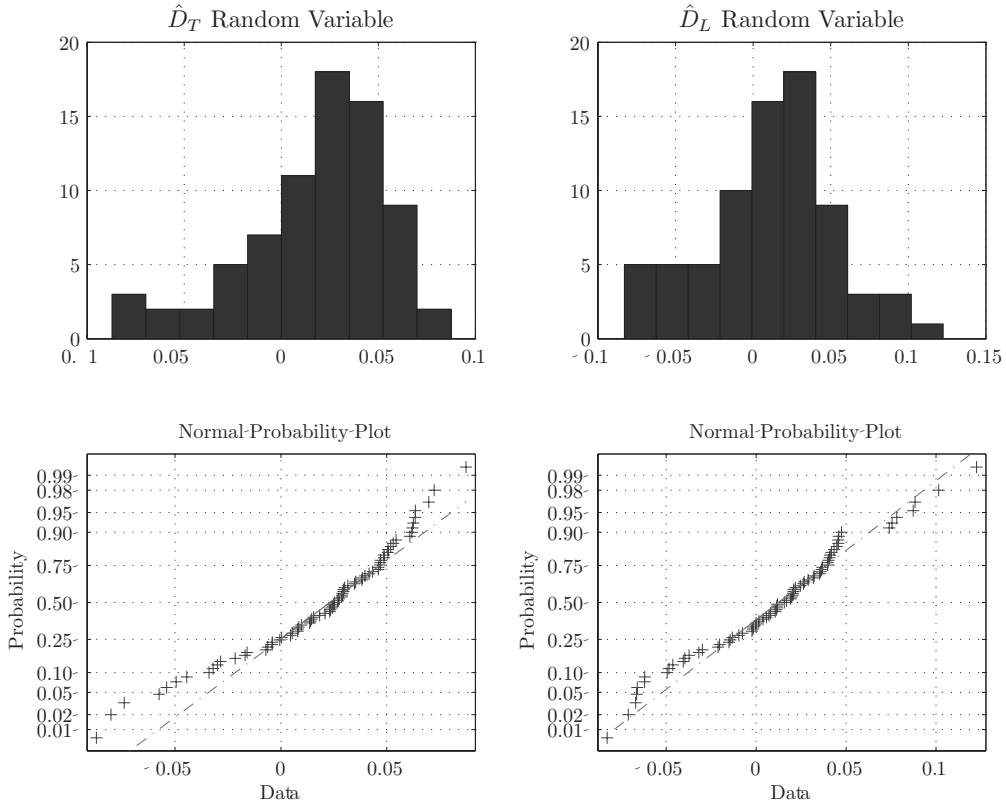

Fig. 5. Histograms and normal probability plots of the maximum likelihood values of the random variables $\hat{D}_T^t$ (left panels) and $\hat{D}_L^t$ (right panels), which allows reproducing the data trajectories.

and there is just one partial autocorrelation coefficient at lag 1 clearly outside the 95% confidence bands. This indicates that the processes are very likely to correspond to moving autoregressive processes of order one. Fitting both ARMA$(1,0)$ models to the times series $\hat{\boldsymbol{z}}^{D_T}$ and $\hat{\boldsymbol{z}}^{D_L}$, the following parameter estimates are obtained: $\hat{\phi}_1^{D_T} = -0.7059$ and $\hat{\phi}_1^{D_L} = -0.6624$. The standard deviation estimates of the residuals are $\hat{\sigma}_\varepsilon^{D_T} = 0.71791$ and $\hat{\sigma}_\varepsilon^{D_L} = 0.71771$, respectively. The p-values obtained from the one-sample Kolmogorov-Smirnov test over the samples $\hat{\boldsymbol{\varepsilon}}^{D_T}/\hat{\sigma}_\varepsilon^{D_T}$ and $\hat{\boldsymbol{\varepsilon}}^{D_L}/\hat{\sigma}_\varepsilon^{D_L}$ are, respectively, 0.42726 and 0.10540, so that the null hypothesis that both samples follow a standard normal distribution is accepted.

Figures 7 and 8 show, respectively, the autocorrelation and partial autocorrelation functions, the normal probability plots, and the histograms related to the ARMA residuals. Note that in both cases the autocorrelation and partial autocorrelation functions for different time lags are within the confidence bands, confirming that the residuals are uncorrelated. Finally, the Ljung-Box lack-of-fit hypothesis test considering the null hypothesis that no serial correlation at the lags 1, 2, 3, 4, and 5 exist has been applied on the residual samples. The p-values obtained for a 5% significance level are (0.55443, 0.55359, 0.59565, 0.60598, 0.72131) for the transversal residuals, and (0.93430, 0.79786, 0.92803,

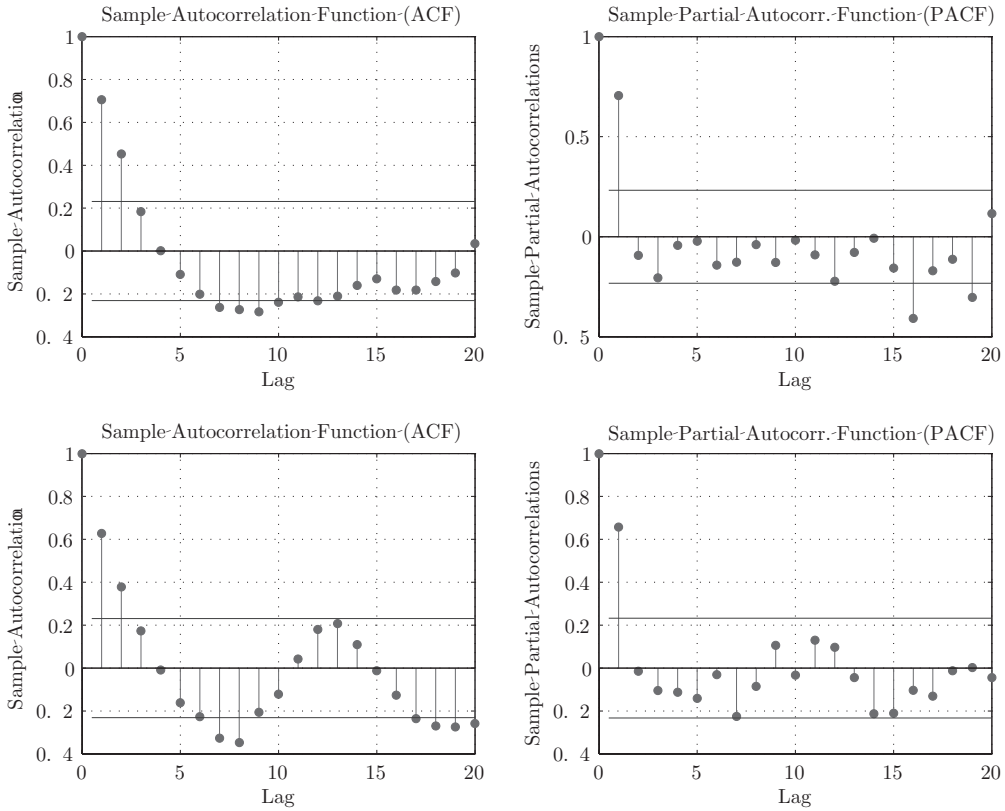

Fig. 6. Autocorrelation and partial autocorrelation functions related to the maximum likelihood values of the random variables $\hat{z}_t^{D_T}$ (panels above) and $\hat{z}_t^{D_L}$ (panels below), which allows reproducing the data trajectories.

0.97716, 0.79897) for the longitudinal residuals. Note that since in all cases the p-values are higher than the significance level 0.05, the null hypothesis is accepted.

4.3 Simulation and validation results

Once the model parameter estimates are obtained and the probability distribution hypothesis are tested, the next step encompasses the validation of the simulation procedure proposed in Section 3.

Initially, we produce 10000 simulated trajectories total using algorithm 3.1, starting from the three known positions at 15:45:00 September 14th 2010, to the locations at 22:00:00 September 14th 2010. The cloud of locations of the simulated trajectories for each of the three buoys are shown in Figure 9.a, i.e. the red, blue and green dots labeled as SIM 1, SIM 2 and SIM 3, respectively. Besides the simulated trajectories, the true trajectories (DATA 1, DATA 2 and DATA 3) and the simulated ones (BESTSIM 1, BESTSIM 2 and BESTSIM 3), which are the closest to the true ones, are also shown. The proximity

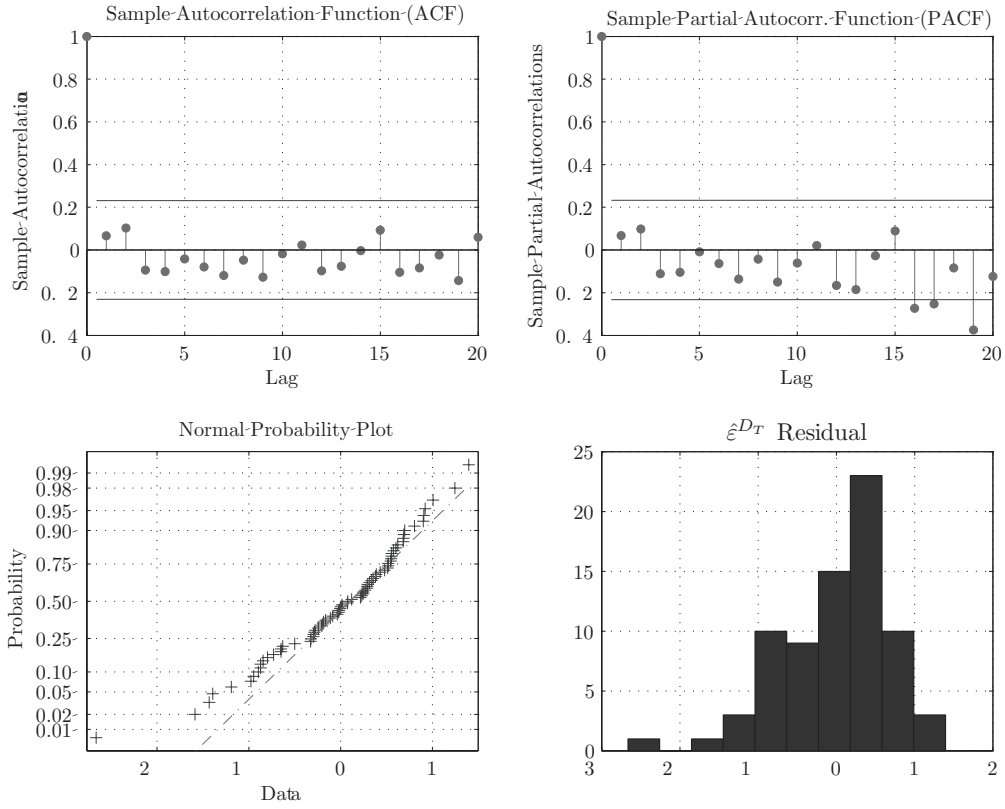

Fig. 7. Autocorrelation and partial autocorrelation functions, normal probability plot and histogram of the residuals $\boldsymbol{\varepsilon}^{D_T}$ obtained after fitting an ARMA$(1,0)$ model given by (23).

measure is calculated using the Euclidean distance between simulated and data trajectories. Note that both deterministic and MLE trajectories correspond to those in Figure 4.

For analyzing the three trajectories more in detail, Figures 9.a, b and c, show the actual trajectories and the contour plots related to the density of points, respectively. The higher the contour value is for each location, the higher the likelihood of the corresponding buoy to go through the location. For this reason they are called "likelihood contour plots". Note that the actual buoy trajectories are in the areas where the model predicted that buoy is likely to go through. These contour plots were constructed merging the information given by the 25 simulated locations for each of the 10000 simulated trajectories.

If instead of using all the information, we use the information related to a particular time step, we can obtain the likelihood contour plot of the location at a given time, as shown in Figures 10.a, b and c. Note that these contour plots could be rescaled to represent probabilities, however the contour values would take very low values. From these results, the following observations are pertinent:

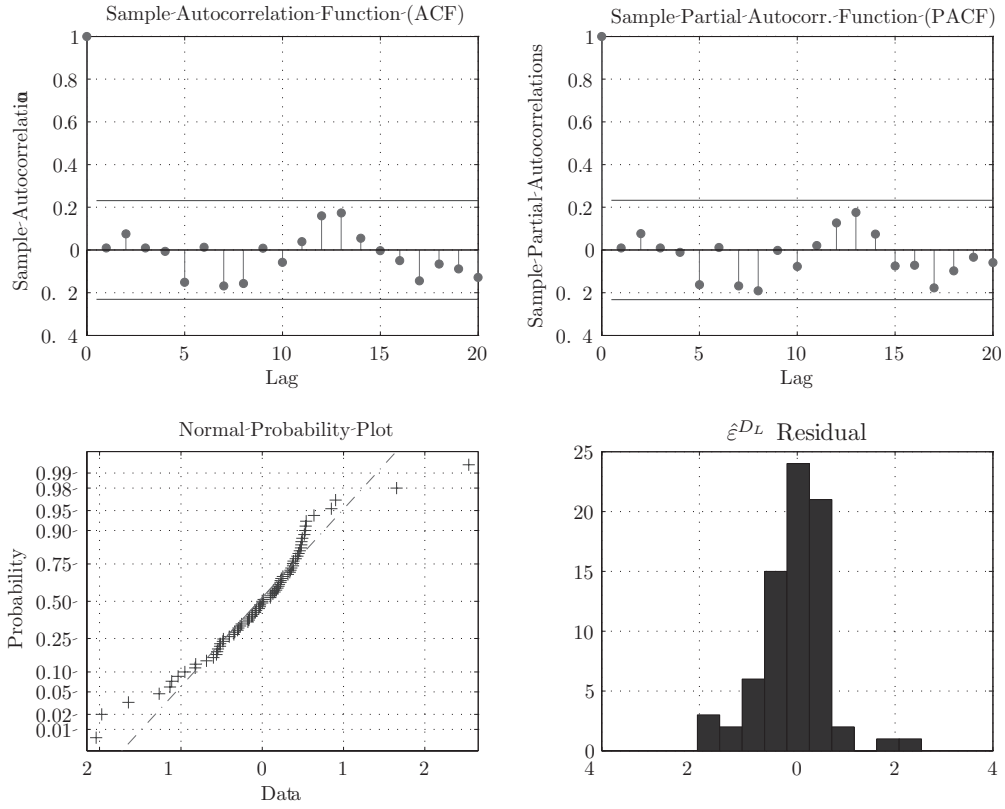

Fig. 8. Autocorrelation and partial autocorrelation functions, normal probability plot and histogram of the residuals $\boldsymbol{\varepsilon}^{D_L}$ obtained after fitting an ARMA$(1,0)$ model given by (22).

(1) The actual trajectory at that time is between the bounds given by the blue dashed line square, which represents the area where there are simulated values. This means that the model covers the actual final location.
(2) The final value is not close to the most likely positions indicated by the contour plot. This could be due to the effects not taking into account, such as leeway velocities due to wind and Stokes drift induced by waves, which may have changed with respect to those during the parameter estimation period.

To further explore the simulation method, we produce additional 10000 simulated trajectories total using algorithm 3.1, starting from the three known positions at the beginning of the buoy exercise at 09:30:00 September 14th 2010 until 22:00:00 September 14th 2010. Analogous results as those in Figure 9 are shown in Figure 11.

Note that for the three trajectories, the true values labeled as DATA 1, DATA 2 and DATA 3, are all within the 1000 likelihood contours, and the trajectories during the parameter estimation period (up to 15:45:00 September 14th 2010) are within the 2500 likelihood contours. This result is reasonable since the true trajectories are the maximum likelihood estimates of the corresponding

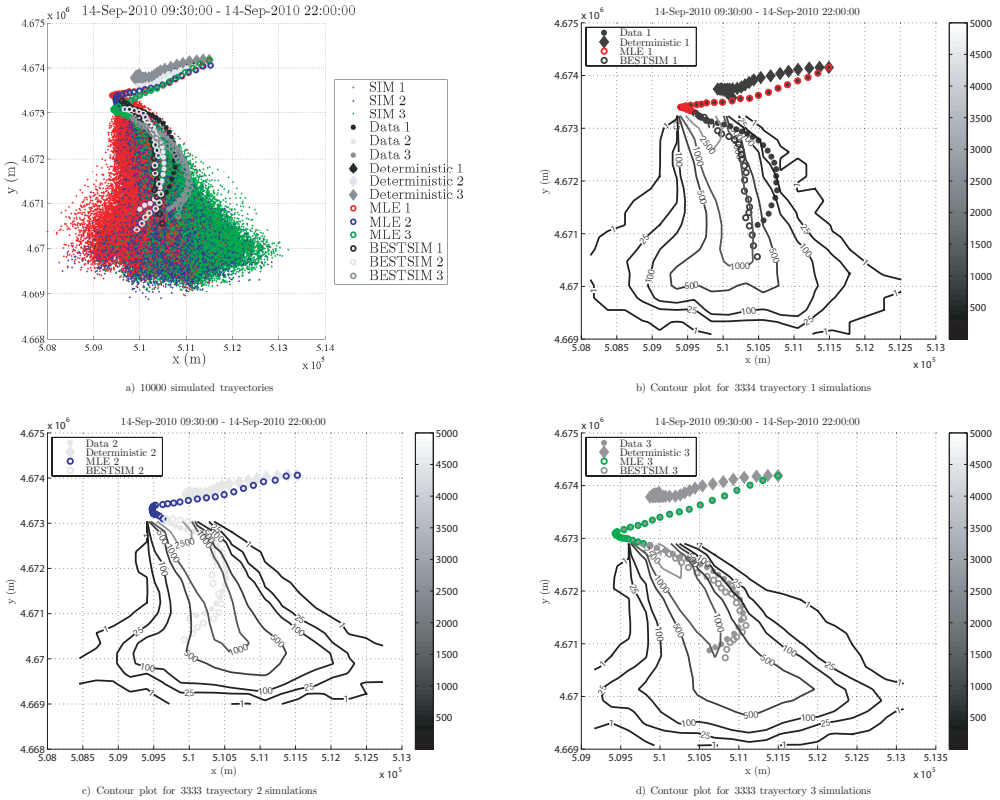

Fig. 9. 10000 simulated trajectories from 15:45:00 September 14th 2010 to 22:00:00 September 14th 2010.

model, and the uncertainty increases when the model is used to forecast.

The increment in uncertainty is also observed in Figure 12, where contour plots of the locations at two different times are shown. First time corresponds to the end of the parameter estimation period, i.e. 15:45:00 September 14th 2010, and the second, to the end of the forecasting period, i.e. 22:00:00 September 14th 2010. Note that the contours increase the diffusion area for the second time. Observe also that the true locations for each buoy and time are within the simulated likelihood contours, which proves the good performance of the proposed methodology.

5 Conclusions

This paper presents an stochastic Lagrangian trajectory model for drifting objects in the ocean. The proposed method has the following advantages:

(1) It allows including different sources of uncertainty by means of their probability density functions.
(2) The parameters of the selected distributions are estimated using the max-

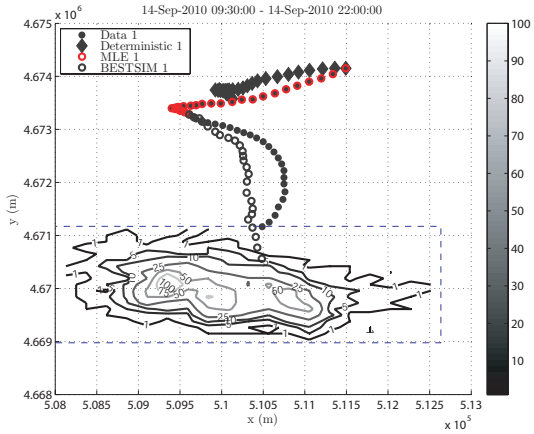

a) Contour plot for 3334 trayectory 1 simulations

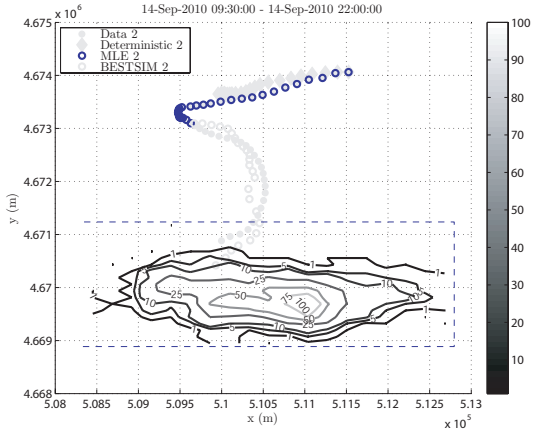

b) Contour plot for 3333 trayectory 2 simulations

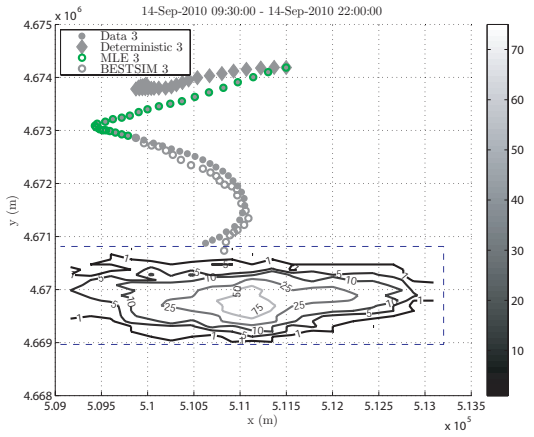

c) Contour plot for 3333 trayectory 3 simulations

Fig. 10. Likelihood contour plots of the simulated trajectories at 22:00:00 September 14th 2010.

imum likelihood method. Particularly, the estimates maximize the likelihood of the model to reproduce the trajectory data.

(3) It allows incorporating the temporal autocorrelation of the random variables involved, through simple ARMA models.

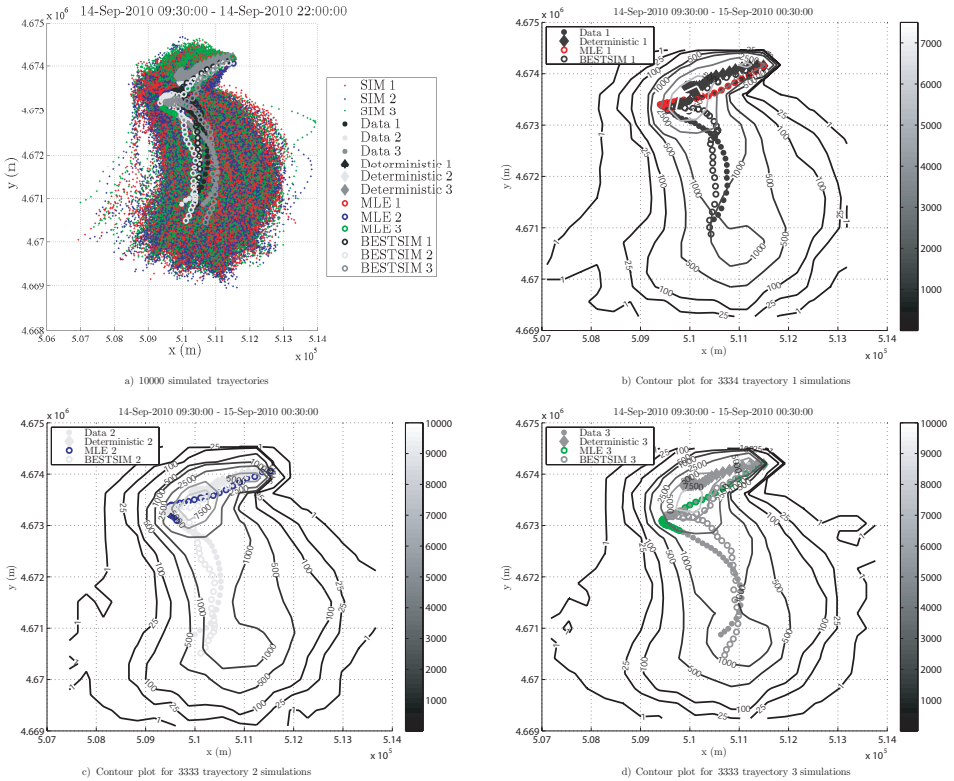

Fig. 11. 10000 simulated trajectories from 9:30:00 September 14th 2010 to 22:00:00 September 14th 2010.

(4) The proposed method provides a rationale criterion for uncertainty quantification. This characteristic is specially useful to compare the effectiveness of different wave climate (currents, winds, waves, etc.) forecasting methods.
(5) In addition, a simple algorithm to simulate different trajectories is given. The simulated trajectories allows calculating the probability density functions (likelihood contour plots) of the locations at different times.

Summarizing, this method constitutes a coherent, simple, and easy to implement stochastic framework to deal with drifting trajectories in the ocean, which is further reinforced by the results obtained from the DRIFTER Project case study. The proposed methodology sets the methodological framework for new applications and further studies, such as, the proposal of more complex probabilistic models, including wind and wave information, or selection of the best model using the Akaike Information Criterion (AIC)(Akaike, 1973), which establishes a compromise between obtaining a good fit and using a simple model.

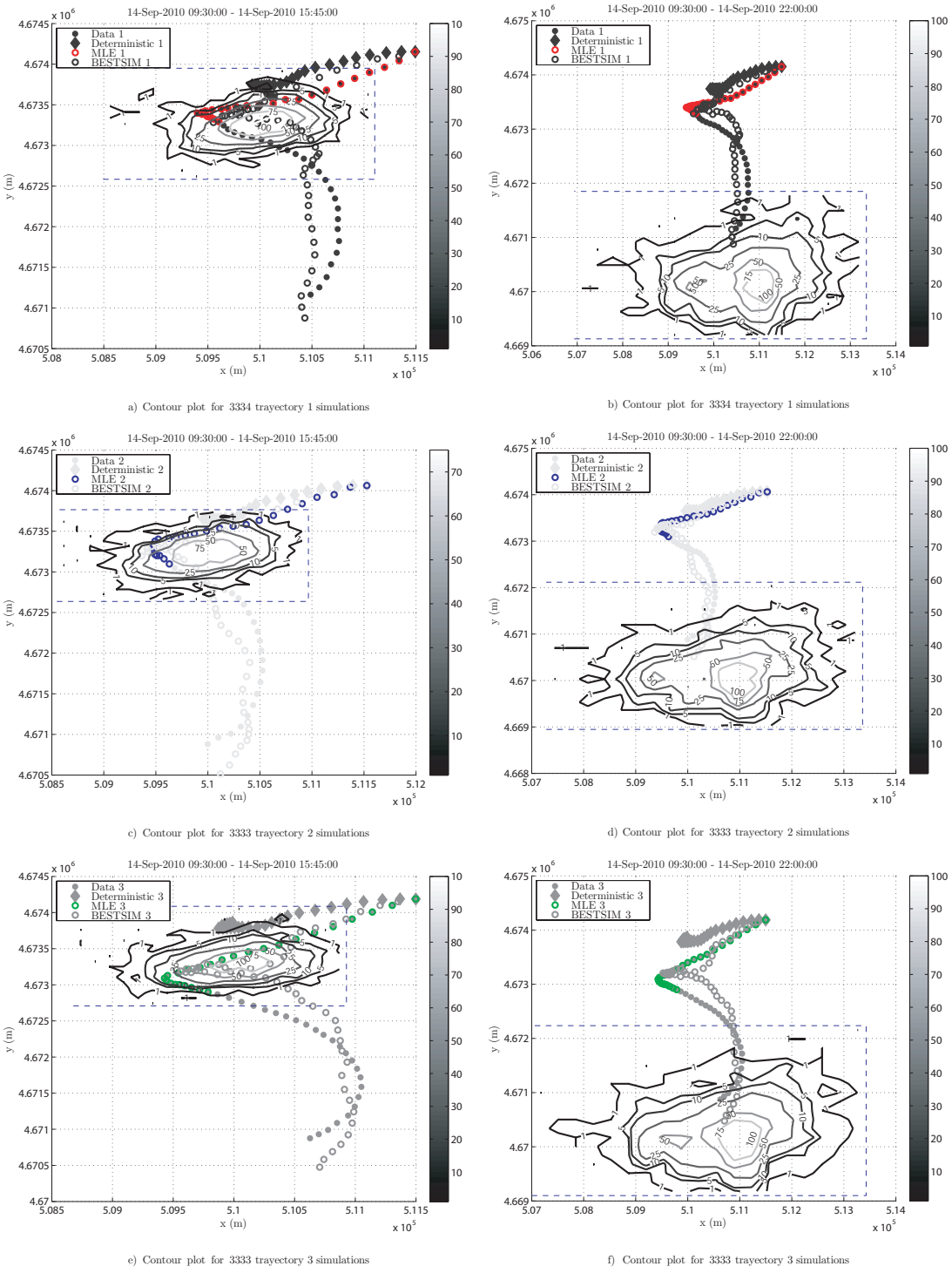

a) Contour plot for 3334 trayectory 1 simulations

b) Contour plot for 3334 trayectory 1 simulations

c) Contour plot for 3333 trayectory 2 simulations

d) Contour plot for 3333 trayectory 2 simulations

e) Contour plot for 3333 trayectory 3 simulations

f) Contour plot for 3333 trayectory 3 simulations

Fig. 12. Likelihood contour plots of the simulated trajectories at: i) 15:45:00 September 14th 2010 and ii) 22:00:00 September 14th 2010.

6 Acknowledgments

This work was partly funded by projects “GRACCIE” (CSD2007-00067, Programa Consolider-Ingenio 2010) and “AMVAR” (CTM2010-15009) from Span-

ish Ministry MICINN, by project C3E (200800050084091) from the Spanish Ministry MAMRM and by project MARUCA (E17/08) and OCTOPOS from the Spanish Ministry MF. R. Mínguez is also indebted to the Spanish Ministry MICINN for the funding provided within the "Ramon y Cajal" program. We also thank DRIFTER, INTECMAR and QUALITAS for the data provided for this research.

References

Abascal, A. J., Castanedo, S., Fernández, V., Ferrer, M. I., Medina, R., 2011a. Backtracking drifting objects using surface currents from High-Frequency (HF) radar technology. In: OCEANS '11 MTS/IEEE. Oceans of Energy for a Sustainable Future. Vol. –. pp. –.

Abascal, A. J., Castanedo, S., Fernández, V., Medina, R., 2011b. Backtracking drifting objects using surface currents from High-Frequency (HF) radar technology. Ocean Dynamics(submitted).

Abascal, A. J., Castanedo, S., Medina, R., Losada, I. J., Alvarez-Fanjul, E., 2009a. Application of HF radar currents to oil spill modelling. Marine Pollution Bulletin 58, 238–248.

Abascal, A. J., Castanedo, S., Méndez, F. J., Medina, R., Losada, I. J., 2009b. Calibration of a Lagrangian transport model using drifting buoys deployed during the Prestige oil spill. Journal of Coastal Research 25 (1), 80–90.

Akaike, H., 1973. Information theory and an extension of the maximum likelihood principle. In: Petrov, B. N., Csáki, F. (Eds.), Proceedings 2nd International Symposium on Information Theory. Akadémia Kiadó, Budapest, pp. 267–281.

Allen-Perkins, S., Montero, P., Ayensa, G., 2010. Testing and application of buoys to follow up spills. In: Drifter Workshop. Vigo (Spain).

ASCE, 1996. State-of-the-art review of modeling transport and fate of oil spills. J. Hydraul. Eng. 122 (11), 594–609.

Beegle-Krause, C., 1999. GNOME: NOAA's next-generation spill trajectory model. In: OCEANS '99 MTS/IEEE. Riding the Crest into the 21st Century. Vol. 3. pp. 1262–1266.

Berloff, P. S., McWilliams, J. C., march 2002. Material transport in oceanic gyres. Part II: Hierarchy of stochastic models. J. Phys. Oceanogr. 32, 797–830.

Box, G. E. P., Jenkins, G. M., Reinsel, G. C., 1994. Time Series Analysis: Forecasting and Control. Prentice-Hall International, New Jersey, NJ.

Brockwell, P. J., Davis, R. A., 1991. Time series: Theory and methods, 2nd Edition. Springer-Verlag, New York, NY.

Brooke, A., Kendrick, D., Meeraus, A., Raman, R., 1998. GAMS: A user's guide. GAMS Development Corporation, Washington.

Castanedo, S., Medina, R., Losada, I. J., Vidal, C., Mendez, F. J., Osorio, A.,

A, J. J., Puente, A., 2006. The Prestige oil spill in Cantabria (Bay of Biscay). Part I: Operational forecasting system for quick response, risk assessment and protection of natural resources. J. Coast. Res. 22 (6), 1474–1489.

Coleman, T. F., Li, Y., 1994. On the convergence of reflective newton methods for large-scale nonlinear minimization subject to bounds. Mathematical Programming 67 (2), 189–224.

Coleman, T. F., Li, Y., 1996. An interior, trust region approach for nonlinear minimization subject to bounds. SIAM Journal on Optimization 6, 418–445.

Daniel, P., Marty, F., Josse, P., Skandrani, C., Benshila, R., 2003. Improvement of drift calculation in Mothy operational oil spill prediction system. In: Proceedings of the 2003 International Oil Spill Conference. Washington, D.C.

Griffa, A., 1996. Stochastic modelling in physical oceanography. In: Adler, R., Muller, P., Rozovskii, B. (Eds.), Applications of stochastic particle models to oceanographic problems. Birkhauser, Boston, pp. 113–128.

Hackett, B., Breivik, O., Wettre, C., 2005. Forecasting the drift of objects and substances in the ocean. In: Chassignet, E. P., Verron, J. (Eds.), Ocean Weather Forecasting: An Integrated View of Oceanography. Springer, pp. 507–523.

Harr, M. E., 1989. Probabilistic estimates for multivariate analysis. Appl. Math. Model. 13 (5), 313–318.

Hong, H. P., 1998. An efficient point estimate method for probabilistic analysis. Reliab. Eng. Syst. Saf. 59, 261–267.

Liu, P.-L., Der Kiureghian, A., 1986. Multivariate distribution models with prescribed marginals and covariances. Probabilistic Engineering Mechanics 1 (2), 105–112.

Massey, F. J., 1951. The kolmogorov-smirnov test for goodness of fit. Journal of the American Statistical Association 46 (253), 68–78.

Morales, J. M., Pérez-Ruiz, J. P., November 2007. Point estimate schemes to solve the probabilistic power flow. IEEE Trans. Power Syst. 22 (4), 1594–1601.

Murtagh, B. A., Saunders, M. A., 1978. Large-scale linearly constrained optimization. Mathematical Programming 14, 41–72.

Murtagh, B. A., Saunders, M. A., 1998. MINOS 5.5 Users Guide. Report SOL 83-20R SOL 83-20R, Department of Operations Research, Stanford University, Stanford, California.

Rixen, M., Ferreira-Coelho, E., 2007. Operational surface drift prediction using linear and non-linear hyper-ensemble statistics on atmospheric and ocean models. Journal of Marine Systems 65, 105–121.

Rixen, M., Ferreira-Coelho, E., Signell, R., 2008. Surface drift prediction in the Adriatic Sea using hyper-ensemble statistics on atmospheric, ocean and wave models: Uncertainties and probability distribution areas. Journal of Marine Systems 69 (1–2), 86–98.

Rosenblueth, E., October 1975. Point estimates for probability moments. Proc. Nat. Acad. Sci. 72, 3812–3814.

Rubinstein, B. V., 1981. Simulation and the Monte Carlo Method. John Wiley & Sons, New York.

Sebastião, P., Guedes Soares, C., 2006. Uncertainty in predictions of oil spill trajectories in a coastal zone. Journal of Marine Systems 63, 257–259.

Sebastião, P., Guedes Soares, C., 2007. Uncertainty in predictions of oil spill trajectories in open sea. Ocean Engineering 34, 576–584.

Spaulding, M. L., Howlett, E., Anderson, E., Jayko, K., 1992. OILMAP: A global approach to spill modelling. 15th Annual Arctic and marine Oilspill Program, Technical Seminar, Edmonton, Aberta, Canada.

Varela, R., 2010. Implementación de un sistema radar de alta frecuencia en la Ría de Vigo. características fundamentales. In: I Encuentro Oceanografía Física Española. Barcelona (Spain).

Wolfe, P., 1963. Methods of nonlinear programming. In: Graves, R. L., Wolfe, P. (Eds.), Recent Advances in Mathematical Programming. McGraw-Hill, New York, pp. 76–77.